

Protein Immobilisation on Perpendicularly Aligned Gold Tipped Nanorod Assemblies†

Catriona O'Sullivan^a, Suzanne Crilly^a, Fathima R. Laffir^a, Ajay Singh^{ab}, Edmond Magner^{*ab} and Kevin M. Ryan^{ab*}

⁵ Received (in XXX, XXX) Xth XXXXXXXXXX 200X, Accepted Xth XXXXXXXXXX 200X

First published on the web Xth XXXXXXXXXX 200X

DOI: 10.1039/b000000x

A multi component assembly consisting of the redox protein cytochrome c (cyt c) immobilised onto vertically aligned gold tipped semiconductor nanorods is described. Cyt c was successfully immobilised using a thiol linker. A faradaic response demonstrated that the protein is electroactive in this ultra high density array.

Bottom up assembly of nanoscale structures has the potential to allow discrete properties of each unit such as size tunable band gap (semiconductor), plasmon resonance (metal) or biological species (molecular) to be collectively integrated in high density for scalable applications. Recently, semiconductor nanorods have been shown to assemble into vertically aligned supercrystals from solution over device useable centimeter scale areas.¹ Gold tips can be selectively attached to the end facets of each rod by a facile spin cast process showing that more complex heterojunctions can be formed in high density using the perpendicular nanorod array as the host architecture.² This sequential attachment route is more attractive than preforming of the heterostructure and its subsequent assembly which requires intermediate steps of ligand exchange.³

Here we demonstrate the formation of high density arrays of three component semiconductor-metal-molecular conjugates by selective immobilisation of cyt c via a thiol linker ($\text{Au}^0\text{-S}$) to the gold metal tip. Much work has been described in the immobilization of proteins to various surfaces with modified gold surfaces being particularly common as such surfaces can promote direct electron transfer.⁴ Cyt c is a single heam electron transport protein that is readily available, stable and widely used as a model for larger, more complex systems.⁵ Cyt c undergoes a characteristic electrochemical response when immobilized on a substrate, ensuing that attachment to the array can be easily verified.⁶

Fig. 1a and Fig. 1b show high resolution scanning electron microscopy (HRSEM) and high resolution transmission electron microscopy (HRTEM) images of the inorganic component in the assembly. The SEM side view image (Fig. 1a) shows the vertically aligned nanorods which were electrophoretically deposited onto large 2 cm × 1 cm ITO coated glass substrates, (see ESI†, Fig. S1 and S2). Nanorods of 100 nm in length were obtained by controlled oriented attachment of as synthesised nanorods 35 nm in length.⁷ The nanorods are bound to the substrate at the end facets and are separated from each other (~ 2 nm) by interdigitated long-chain octadecyl phosphonic acid ligands. The resulting

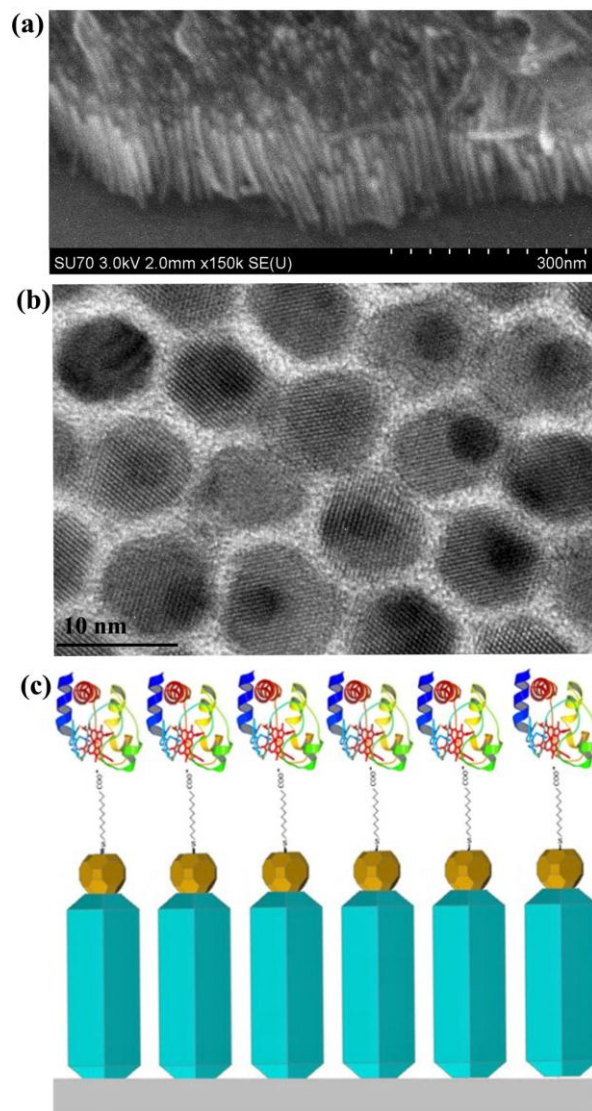


Fig. 1. Side view HRSEM image of (a) perpendicularly aligned nanorods (b) HRTEM top down image of gold tipped nanorods (c) schematic showing the bottom up assembly process consisting of gold tipped nanorods on an ITO substrate

perpendicularly aligned nanorods were spun cast with a solution of gold chloride to grow a single gold tip on each rod in the array (Fig. 1b and ESI†, Fig. S3). The procedure was optimized to form individual gold tips of 3 nm in size, on

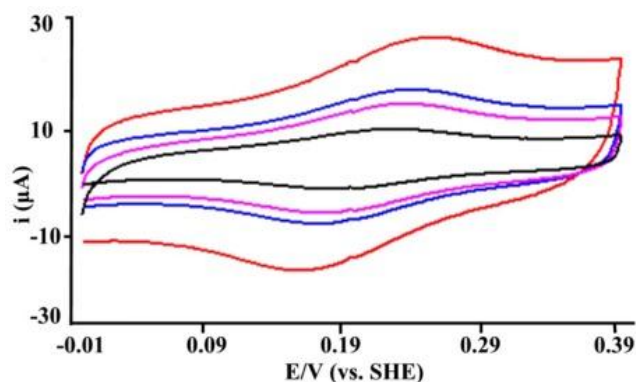
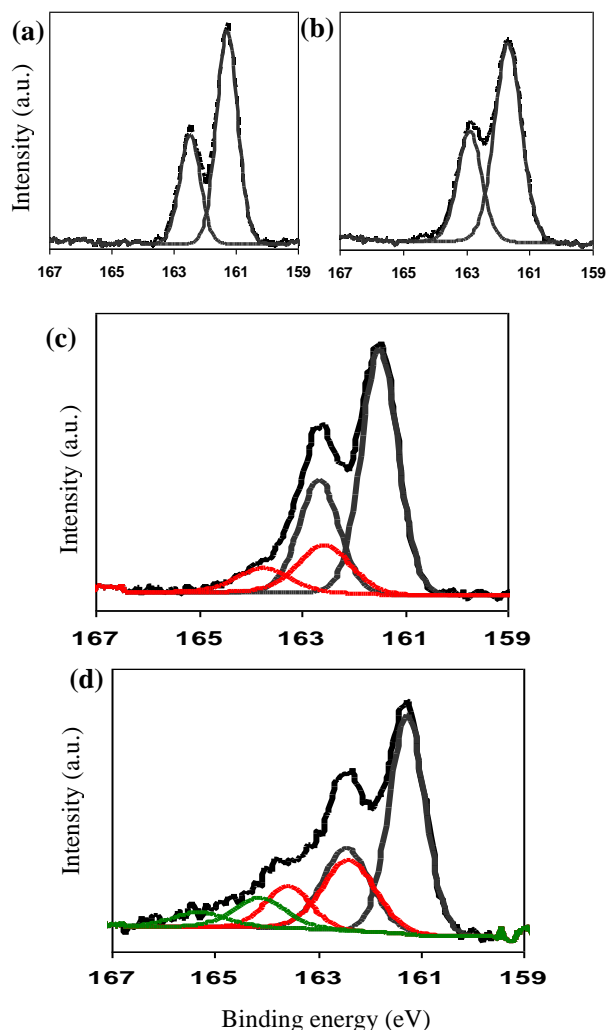


Fig. 2. Cyclic voltammogram (C.V) of cyt c immobilisation via HS(CH₂)₁₀COOH/HS(CH₂)₇OH onto gold tipped nanorods in 10 mM phosphate buffer, pH 7.4 at 20 mVs⁻¹ (—), 40 mVs⁻¹ (—), 50 mVs⁻¹ (—) and 100 mV s⁻¹ (—).

the terminating facet.⁸ (Fig. 1b and ESI†, Fig. S4) A 2D schematic of the proposed nanorod-gold-thiol-cyt c conjugate is shown in figure 1c. Cyt c is ca. 3 nm in size, closely matching that of the gold nanoparticle tips (Fig. 1b). The similar sizes of the tip and protein in addition to close packing of the gold tipped nanorods means steric factors should favor the adsorption of a single protein on each tip.

As the processes of gold tip formation introduces additional insulating surfactants to the as deposited nanorods, the excess surfactant was removed using a 1:1 H₂:O₂ plasma prior to protein immobilisation. The resultant CdS-Au array showed a well-defined faradaic response in the presence of ferricyanide (E^o = 432 mV vs. SHE and ΔE_p = 111 mV at v = 20 mVs⁻¹). This response is quasi-reversible and demonstrates that electron transport is occurring axially through the heterostructure as no nanorod to nanorod charge transfer is possible due to the long chain phosphonic spacers which are electrically insulating.¹ Plots of i_{pa} and i_{pc} vs. (scan rate)^{1/2} (v)^{1/2} were linear and indicative of a diffusion controlled electrochemical process. The electrochemical response of cyt c was examined using a mixed layer of HS(CH₂)₁₀COOH/HS(CH₂)₇OH on gold tipped nanorod arrays. Mixed carboxylate/hydroxyl layers have been shown to provide faster and more reversible kinetics than their acid only equivalents.⁹ A well defined faradaic response was observed indicating that cyt c is electroactive on the perpendicularly aligned array after immobilization (Fig. 2). The values of E^o (257 mV vs. SHE) and ΔE_p (39 mV) (v = 20 mVs⁻¹) were in good agreement with literature values indicating that the protein was electroactive.¹⁰ Plots of i_{pa} and i_{pc} vs. scan rate were linear indicating that cyt c was immobilized on the Au tips on the semiconductor nanorod array (see ESI†, Fig. S5). The surface coverage (Γ*) of cyt c was approximately one monolayer suggesting that the most likely structure is attachment of a single protein molecule to each nanorod hybrid column given the similar sizes of the gold tip and the protein as expected. Perpendicular alignment of the nanorods is a critical factor in achieving a faradaic response for cyt c, with no faradaic

Fig3. XPS spectra of S 2p



for as synthesized CdS nanorods (a), gold tipped CdS nanorods (b), gold tipped CdS nanorods containing thiol linkages (c) and gold tipped CdS nanorods with thiol linkage and cyt c (d)

response observed for nanorods lying parallel to the substrate (see ESI†, Fig. S6). The apparent electron transfer rate constant, k_{et}, was determined using Laviron's model and had a value of k_{et} = 0.7 s⁻¹ at 25 °C in aqueous buffer which is in agreement with literature values.¹¹ The modified electrodes were stored in phosphate buffer, pH 7.4 at 4-6 °C and remained fully functional for several weeks.

XPS (x-ray photoelectron spectroscopy) was performed at each stage in the bottom up assembly process to confirm the sequential addition of each component. The sulphur (S) 2p photoelectron transitions, which appear as doublets with an intensity ratio of 1:2 for 2p_{1/2}:2p_{3/2}, were examined at each stage of the process due to the increasing amounts of S. Fig. 3a shows the S 2p_{3/2} peak appearing at a binding energy of 160.3 eV corresponding to sulfide in the CdS semiconductor nanorod.¹² This peak remains unchanged when gold tips were grown on the nanorod (Fig. 3b). The chemisorption of thiols to the gold tipped nanorods shows the presence of an additional doublet peak at 162.4 eV, Fig. 3c, which can be

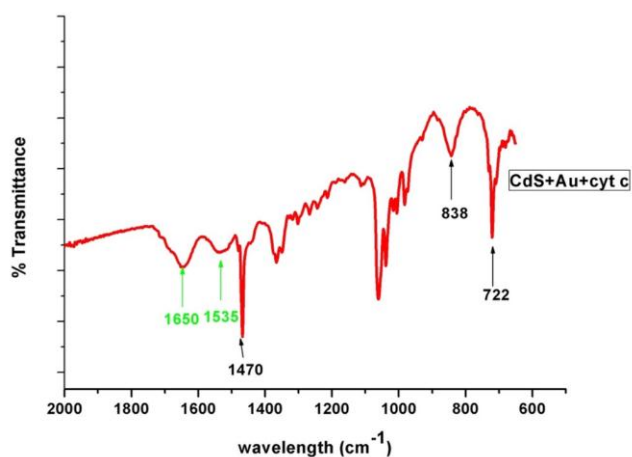


Fig 4. FTIR spectra of CdS nanorods + Au tips + cyt c

assigned to the thiolate sulfur bound to Au.¹³ On immobilization of the protein on the thiol bound gold tipped semiconductor nanorods, Fig 3d, a third state for sulfur was observed at a higher binding energy of 164.0 eV which can be assigned to sulfur linkages present in the protein.¹⁴ The ratio of Au/thiolate remains constant in Fig 3c and d supporting the sequential construction of the proposed structure. The appearance of N 1s and a significant contribution to C 1s peaks in the latter nanostructure also signifies the presence of protein where the N 1s is attributed to amino and peptide links of the adsorbed protein and C 1s to the presence of C—O, carboxyl and peptide carbons within the ensemble (see ESI†, Fig. S7-S8).¹²

The immobilisation of cyt c on the perpendicularly aligned gold terminated nanorod arrays was further confirmed by Fourier transform infrared (FT-IR) spectroscopy (Fig. 4). Fig. 4 shows the combined IR spectra for CdS, Au, thiol and cyt c. The characteristic amide I peak at 1650 cm⁻¹ and amide II at 1535 cm⁻¹ bands confirms the presence of cyt c.¹⁵ The vibration band of the -NH₂ group at 838 cm⁻¹ is indicative of a combination of cyt c and dodecylamine, the ligand utilised for the controlled gold tip growth. The band at 722 cm⁻¹ further confirms the presence of the long chain (CH₂)_n (n ≥ 7) of dodecylamine and the additional bands occurring at ~ 1470 cm⁻¹ can be assigned to the methylene scissoring. The presence of the thiol linkers was confirmed by the weak S-H stretching absorption peak at 2565 cm⁻¹, see ESI† Fig. S9. The S-H stretching signal is generally weak for thin film samples. The vibration frequency between 1000-1200 cm⁻¹ can be attributed to phosphine oxide (P=O) and the band at ~900 cm⁻¹ due to hydroxide (P-OH) to the surface ligands on CdS, (ODPA/TOPO), see ESI† Fig. S10 for a full CdS nanorod spectra.

In conclusion we show the sequential bottom up formation of vertically aligned arrays of semiconductor nanorod-metal-molecule conjugates on a substrate. In this study cyt c is used as a model biomolecule highlighting that a reaction (redox) occurring at the protein can be detected at the substrate through the nanostructured array. While the demonstrated response shown here is collective, the hierarchical structure allows the possibility of local connection to an individual or small group of columnar nanoconjugates for discrete feedback

from a single molecule. This opens up opportunities for multicomponent biosensing with resolution at the nanoscale or molecular computing where on/off behaviour in the molecule (light or chemically activated) is the switching component for nanoelectronics.¹⁶

This work was supported by Science Foundation Ireland (SFI contract No. 06/IN.1/185) and the HEA funded programme INSPIRE. Funding and support from Intel Ireland is acknowledged under the Irish Research Council for Science, Engineering and Technology embark initiative to CO'S. The authors thank Abbey Moulding Contractors, Abbeyfeale, Limerick, for high precision engineered electrodes for nanorod deposition.

Notes and references

- ^a *Materials and Surface Science Institute (MSSI) and Department of Chemical and Environmental Sciences*
- ^b *SFI-Strategic Research Cluster in Solar Energy Research, University of Limerick, Limerick, Ireland;*
- *Corresponding authors to whom correspondence should be addressed E-mail: kevin.m.ryan@ul.ie, edmond.magner@ul.ie Tel: +353 61213167
- † Electronic Supplementary Information (ESI) available: Experimental detail of the process, photograph, SEM, TEM, CV, XPS and FT-IR analysis. See DOI: 10.1039/b000000x/
1. Ahmed, S.; Ryan, K. M. *Chem. Comm.* 2009, 6421; Sanyal A, Bala, T., Ahmed, S., Singh, A., Piterina, A. V., McGloughlin, T., Ryan K.M. *J. Mat. Chem* 2009, **20**, 7875; Singh, A., Gunning, R. D., Sanyal, A. Ryan, K. M. *Chem Comm*, 2010, **46**, 7193.; Baker, J. L.; Widmer-Cooper, A.; Toney, M. F.; Geissler P. L. Alivisatos A. P. *Nano Lett*, 2010, **10**, 195.
2. O'Sullivan, C.; Ahmed, S.; Ryan, K. M. *J. Mater. Chem.* 2008, **18**, 5218;
3. Mokari, T.; Rotherberg, E.; Popov, I.; Costi, R.; Banin, U., *Science* 2004, **304**, 1787-1790; Zhao, N., Liu, K., Greener, J., Nie,, Z. H. Kumacheva, E., *Nano lett.* 2009, **9**, 3077
4. Medintz, I. *Nat Mater* 2006, 842.;
5. Davis, K. L.; Drews, B. J.; Yue, H.; Waldeck, D. H.; Knorr, K.; Clark, R. A. *J. Phys. Chem. C* 2008, **112**, 6571.; Brayer, G. D.; Murphy, M. E. P. *Cytochrome c: A Multidisciplinary approach*; University Science Books: California, 1996.
6. Crilly, S., Magner, E. *Chem. Comm.* 2009, **5**, 535
7. O'Sullivan, C., Gunning, R. D., Sanyal, A., Barrett, C. A., Geaney, H., Laffir, F. R., Ahmed, S., Ryan, K. M., *J. Am. Chem. Soc.*, 2009, **131**, 12250; Gunning, R. D., O'Sullivan, C., Ryan, K. M., *Phys.Chem.Chem.Phys.*, 2010, **12**, 12430
8. O'Sullivan, C., Gunning, R. D. Barrett, C. A. Singh A., Ryan, K. M. *J. Mater. Chem.* 2010, **20**, 7875
9. El Kasmi, A.; Wallace, J. M.; Bowden, E. F.; Binet, S. M.; Linderman, R. J. *J. Am. Chem. Soc.* 1998, **120**, 225.
10. Clark, R. A.; Bowden, E. F. *Langmuir* 1997, **13**, 559.; Battistuzzi, G.; Borsari, M.; Cowan, J. A.; Ranieri, A.; Sola, M. *J. Am. Chem. Soc.* 2002, **124**, 5315.
11. Laviron E. *J. Electroanal Chem.* 1979, **101**, 19.
12. Moulder J.F., Stickle W.F., Sobol P.E., Bomben K.D., *Handbook of X-Ray Photoelectron Spectroscopy*, Perkin-Elmer Corporation Physical Electronics Division, 1992
13. Tai, Y.; Shaporenko, A.; Rong, H. T.; Buck, M.; Eck, W.; Grunze, M.; Zharnikov, M. *J. Phys. Chem. B* 2004, **108**, 16806.
14. NIST-XPS database, version 3. (<http://srdata.nist.gov/xps/>)
15. Silverstein, R. M. Webster, F. X., Kiemle, D. J. *Spectrometric Identification of Organic Compounds* (seventh edition) 2004
16. Qian, Z.; Tan, T. C. *Chem. Eng. Sci.* 1998, **53**, 3281; Dickson, R. M.; Cubitt, A. B.; Tsien, R. Y.; Moerner, W. E. *Nature* 1997, **388**, 355.; Ladd, T. D.; Jelezko, F.; Laflamme, R.; Nakamura, Y.; Monroe, C.; O'Brien, J. L. *Nature* 2010, **464**, 45.